

The Location, Structure, and Role of MoO_x and MoC_y Species in Mo/H-ZSM5 Catalysts for Methane Aromatization

Wei Li¹, George D. Meitzner², Young-Ho Kim¹, Richard W. Borry¹, and Enrique Iglesia¹

1 Department of Chemical Engineering, University of California at Berkeley,
Berkeley, CA 94720

2 Edge Analytical, Inc., 2126 Allen Blvd., Middleton, WI 53562

The location, structure, and role of MoO_x and MoC_y species in solid-state exchanged Mo/H-ZSM5 catalysts were probed by infrared, UV-visible, and X-ray absorption (XAS) spectroscopy, and by time-resolved mass spectrometric measurements of the initial products of methane reactions. UV-vis spectra of MoO₃/H-ZSM5 mixtures showed a shift in edge to higher energies during treatment in air at 773 K, showing the dispersion of MoO₃ crystallites as smaller domains. The intensity of the OH infrared band at 3610 cm⁻¹ decreased only above 773 K, indicating that Mo⁺⁶ exchange occurs only after MoO₃ dispersion on external zeolite surfaces. The amount of H₂O evolved during exchange and the intensity decrease for the OH band give similar values for the residual OH density and these values indicate that each Mo⁺⁶ replaces one H⁺. Analysis of XAS showed that Mo species exist as (Mo₂O₅)⁺² dimers interacting with two exchange sites in all samples with Mo/Al_F ratios < 0.4. *In situ* XAS detected the reduction and carburization of these dimers during CH₄ reactions at 930-973 K, concurrently with an increase in methane aromatization rates. Infrared OH bands became weaker during this process, indicating that reduction-carburization processes do not remove Mo species from exchange sites to re-form OH groups. The rate of hydrocarbon formation increased as O-atoms (O/Mo=2.5) are removed from (Mo₂O₅)⁺² to form MoC_y species detected by XAS, which remain isolated and retain bonding to framework oxygens.

1. INTRODUCTION

Mo/H-ZSM5 catalysts convert CH₄ to aromatics with high selectivity [1-5]. Similar catalyst performance has been reported using samples prepared via aqueous exchange, impregnation, and solid-state exchange procedures [4, 6, 7], suggesting that MoO_x species become mobile and form thermodynamically stable structures during treatment in air > 773 K, irrespective of the method of deposition or the precursor identity. Our recent studies identified the presence of (Mo₂O₅)⁺² dimers interacting with two exchange sites after treatment of MoO₃/H-ZSM5 physical mixtures in air at 773-973 K [7, 8]. These (Mo₂O₅)⁺² species undergo reduction and carburization reactions in CH₄ at 950 K to form MoC_y species [6, 9, 10]. The number of MoC_y species and the rate of CH₄ conversion to aromatics increased concurrently during contact with CH₄ at 950 K, suggesting that CH₄ reactions require MoC_y active sites. The location, structure, and role of these carbidic species and the thermodynamic nature of the exchanged (Mo₂O₅)⁺² dimers remain unclear. Here, we report *in situ* spectroscopic studies (IR, UV-vis, and XAS) that address the location, structure, and role of MoO_x precursors and of MoC_y sites in samples prepared by solid-state exchange methods.

2. EXPERIMENTAL METHODS

Mo/H-ZSM5 samples (2% wt. and 4% wt. Mo before treatment) were prepared via solid-state exchange using physical mixtures of MoO₃ and H-ZSM5 (Si/Al = 14.5, Zeochem) [7, 8]. The samples were treated in flowing dry air (120 ml min⁻¹) at 623 K (10 K min⁻¹, 6 h hold) and 773 K (10 K min⁻¹, 6 h hold) and 973 K (10 K min⁻¹, 0.5 h hold). After exchange, the samples contain 2.0 % wt. and 3.6 % wt. Mo, corresponding to Mo/Al ratios of 0.20 and 0.37, respectively; they will be referred to as Mo-2 and Mo-4. Infrared spectra were obtained using a Mattson infrared spectrometer with a diffuse reflectance accessory. UV-vis spectra were measured on a Cary 4 spectrometer using a similar diffuse reflectance accessory. X-ray absorption spectra were measured on beamline 4-1 at the Stanford Synchrotron Radiation Laboratory. Spectra were measured in transmission mode with Ar in the ion chambers. A spectrum of Mo foil was simultaneously measured in order to calibrate the monochromator. The analysis of the spectra was carried out using WINXAS [11] and FEFF software [12]. The details of sample preparation and data analysis are reported elsewhere [8].

3. RESULTS

3.1. MoO_x Species

The density and location of exchanged cations in ZSM5 samples markedly affects their chemical and catalytic behavior. The density of residual hydroxyls after exchange can be measured by infrared and by D₂-OH exchange measurements in order to estimate the number of acidic OH groups replaced by cations during exchange. Three types of hydroxyl groups exist in H-ZSM5 samples; they are associated with Brønsted acid sites (Si-OH-Al) [13], extra-framework Al species, and silanol (Si-OH) groups on the outer surface of ZSM5 [14], with corresponding OH stretching bands at 3610 cm⁻¹, 3675 cm⁻¹, and 3745 cm⁻¹, respectively. Figure 1 shows the OH stretching region in the infrared spectra of a MoO₃/H-ZSM5 physical mixture (Mo-2; Mo/Al = 0.20) after treatment in air at several temperatures. The untreated sample shows only physisorbed water (a). After 1 h at 423 K, a band at 3610 cm⁻¹ with a shoulder at 3673 cm⁻¹ appears (b). The intensity of this band increases after a treatment at 623 K for 1 h (c) and then again after 1 h at 773 K (d). The band at 3610 cm⁻¹ and the weaker band at 3740 cm⁻¹ become sharper after treatment at 773 K, but they do not increase in intensity or change in structure after longer times at 773 K (e). Thus, it appears that MoO_x species do not react with OH groups at these temperatures. This is consistent with measurements of water evolution rate during treatment in air [7], which show that exchange occurs between 773 K and 973 K.

UV-vis spectra show, however, that MoO₃ disperses as small domains during air treatment at 773 K. Figure 2 shows the UV-vis spectra for MoO₃ (a), 2% wt. Mo MoO₃/H-ZSM5 physical mixture at room temperature (b), and after *in situ* treatment in air at 773 K for 1 h (c). Both the MoO₃ bulk crystallites and the fresh physical mixture of MoO₃/H-ZSM5 show absorption edges at ~3.3 eV. This absorption edge, however, shifts to a higher energy after treatment at 773 K and merges with absorption features arising from the ZSM5 structure and from adsorbed hydrocarbons. This indicates that MoO₃ crystallites disperse as small domains, resulting in an edge shift to a higher energy, due to quantum confinement effects well established in previous studies [15].

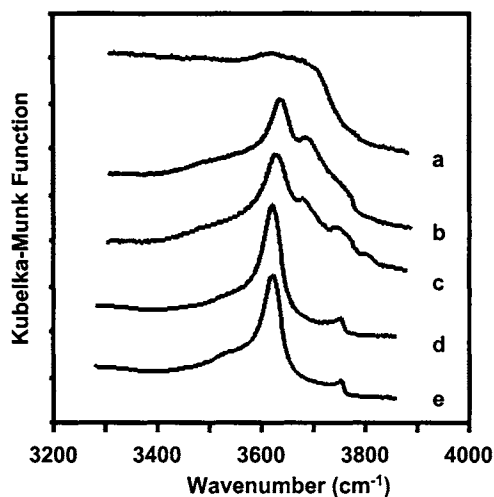


Figure 1. Infrared spectra of a $\text{MoO}_3/\text{H-ZSM5}$ physical mixture (Mo-2; $\text{Mo}/\text{Al}=0.20$) after treatment in flowing dry air at various temperatures. (a) room temperature, (b) 423 K, 1 h, (c) 623 K, 1 h, (d) 773 K, 1 h, (e) 773 K, 3 h. The spectra were measured at room temperature in flowing dry air.

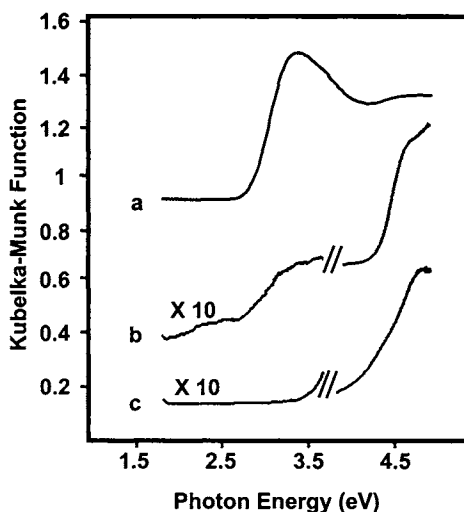


Figure 2. UV-visible diffuse reflectance spectra of MoO_3 (a), $\text{MoO}_3/\text{H-ZSM5}$ physical mixture (2% wt. Mo) at room temperature (b) and after *in situ* treatment in air at 773 K for 1 h (c). The absorbance is expressed as Kubelka-Munk function with MgO as the reference.

Figure 3 shows the infrared spectra for fresh H-ZSM5 (a), H-ZSM5 (b) and Mo/H-ZSM5 (c: Mo-2; d: Mo-4) samples after treatment in air at 973 K, and for Mo/H-ZSM5 treated in CH_4 at 948 K for 2 h (e, f; Mo-2). Fresh H-ZSM5 shows a single band at 3610 cm^{-1} (a), consistent with the predominant presence of acidic hydroxyls and the absence of silanol and extraframework Al sites. After treatment in air at 973 K, H-ZSM5 (b) and Mo/H-ZSM5 (c and d) give additional bands at 3675 cm^{-1} and 3745 cm^{-1} , corresponding to the formation of some extraframework Al and silanol groups respectively, as a result of dealumination. These findings are consistent with a previous study of ZSM5 dealumination [14] and with our earlier ^{27}Al NMR and $\text{D}_2\text{-OH}$ exchange measurements on these samples [7]. They provide evidence of Al mobility at 973 K, a feature that may allow the preferential formation of the Al-Al next nearest neighbor structures required for the anchoring of $(\text{Mo}_2\text{O}_5)^{2+}$ dimers.

The integrated intensity of the 3610 cm^{-1} band reflects the number of Brønsted acid sites in the samples and the extent of exchange in the Mo/H-ZSM5 samples. The intensity of this band for the H-ZSM5 sample treated at 973 K decreased to 68% of the original H-ZSM5, and it also decreased with increasing Mo content, resulting in 55% and 37% of the initial band intensity for the Mo-2 ($\text{Mo}/\text{Al}_F = 0.26$) and Mo-4 ($\text{Mo}/\text{Al}_F = 0.48$) samples, respectively. The calculated number of remaining Brønsted acid sites in the Mo-exchanged samples (Figure 4) agrees with previous measurements by water evolution during exchange and $\text{H}_2\text{-OD}$ exchange reaction [7], and shows a slope of -1 ± 0.2 for the H/Mo ratio, indicating that each Mo replaces one proton.

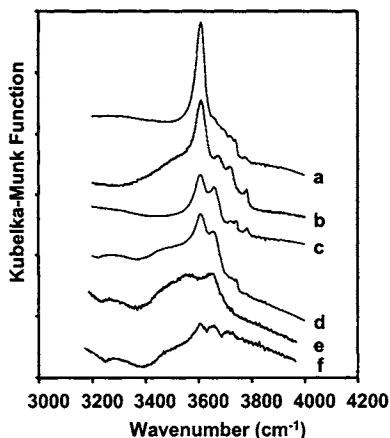


Figure 3. Infrared spectra of H-ZSM5 (a), H-ZSM5 treated at 973 K (b), Mo-2 (c) and Mo-4 (d) exchanged samples, and carburized Mo-2 samples (e and f). Spectra (a) to (d) were measured at room temperature after *in situ* treatment in flowing dry air at 773 K for 1 h, and spectra (e) and (f) were measured at room temperature after *in situ* treatment in flowing Ar and 5% H_2 /Ar at 773 K for 1 h respectively.

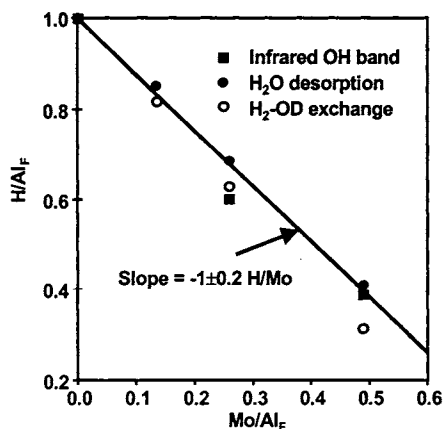


Figure 4. The number of residual OH groups in the Mo-exchanged samples measured using OH infrared band intensity (this work) and using H_2O desorption during exchange and H_2 -OD exchange methods (ref. 7). The Al_F/Al ratio used to calculate the H/Al_F and Mo/Al_F ratios was estimated using the H_2O desorption results of the H-ZSM5 sample.

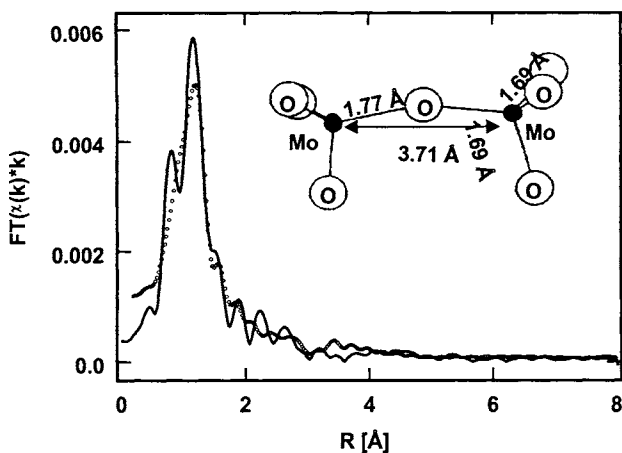


Figure 5. The radial structure function of the measured spectrum (solid line) of the exchanged sample ($Mo/Al_F = 0.26$) and the FEFF fit (symbol o). The model cluster used for the FEFF simulation is shown in the inset.

The proposed structure of $(Mo_2O_5)^{2+}$ requires that framework oxygens connected to Al atoms exist within a distance range of 4.2 - 5.5 nm. Assuming statistical Al distributions at T-sites, the fraction of the Al residing within the distance of another Al for a Si/Al_F ratio of 24 (estimated value after treatment at 973 K) is 0.34 [12]. Therefore, the sample with a Mo/Al_F ratio of 0.26 contains enough Al pairs to accommodate all Mo species as dimers. The sample with a Mo/Al ratio of 0.48, however, would require the migration of Al atoms during thermal treatments in order to accommodate the more than predicted Al-Al pairs. Yet, both samples

The structure of MoO_x precursors formed during solid-state exchange was determined using fine structure analysis by comparing experimental XAS spectra with those obtained using model clusters. A cluster consisting of a $(Mo_2O_5)^{2+}$ dimer with each Mo bonded to a zeolite framework oxygen atom gave excellent agreement with the experimental radial structure function (Figure 5; $Mo/Al_F = 0.26$). The same parameters were able to describe the radial structure function for samples with higher Mo content ($Mo/Al_F = 0.48$) [7], indicating that a single type of MoO_x structure is present over a wide range of Mo/Al ratios (0.1-0.5).

appear to contain a uniform distribution of a single type of MoO_x species. The required mobility is likely to be achieved at the high temperatures required for exchange, along with the detected dealumination. Migration stops when Al sites containing $(\text{MoO}_2\text{OH})^+$ monomers approach a similar Al site and desorption of water occurs by condensation reactions leading to a bridging oxygen in a Mo dimer. The resulting Mo dimers stabilize the structure against further dealumination; they appear to provide a thermodynamic end-point that is kinetically accessible at the high temperatures of the catalyst synthesis process, which leads to identical structures for samples with varying Mo content and preparation method.

3.2. MoC_y Species

Detailed measurements of the products initially formed during reactions of CH_4 at 973 K showed that MoO_x precursor species in exchanged samples reduce and carburize during reaction concurrently with an increase in the rate of aromatics [6, 10]. The resulting MoC_y species provide active sites for C-H activation and hydrocarbon desorption. These species, however, are amorphous and they coexist with carbonaceous deposits formed during CH_4 reactions, making their characterization difficult. Infrared spectroscopy of activated catalysts was used to probe the location of MoC_y (Figure 3, e and f). If $(\text{Mo}_2\text{O}_5)^{2+}$ dimers leave cation exchange sites during reduction, the infrared band associated with acidic hydroxyls (at 3610 cm^{-1}) should reappear during CH_4 reactions. The spectrum of carburized samples, however, showed weaker bands at 3610 cm^{-1} and 3675 cm^{-1} after *in situ* treatment in Ar at 773 K for 1 h (e), and in 5% H_2/Ar at 773 K for 1 h (f) than those in the exchanged $\text{MoO}_x/\text{H-ZSM5}$ precursors. These data suggest that MoC_y species remain anchored at exchange sites during carburization.

Figure 6 shows the near-edge XAS spectra for Mo/H-ZSM5 samples with $\text{Mo}/\text{Al}_F = 0.26$ (Mo-2) after solid-state exchange and after carburization. Spectra for Mo compounds with known structure (MoO_3 , MgMo_2O_7 , and Mo_2C) are also shown. The spectrum of the exchanged sample resembles that of MgMo_2O_7 , which contains two tetrahedral Mo^{+6} centers, but it differs markedly from the spectra of MoO_3 and $(\text{NH}_4)_2\text{Mo}_7\text{O}_{24}$ (not shown), both of which contain at least one octahedral Mo center. The pre-edge feature in the XANES spectra corresponds to a 1s to 4d transition, which is forbidden for centrosymmetric Mo centers. Thus, this feature reflects the presence of tetrahedral Mo centers [16]. The exchanged sample was carburized *in situ* at ca. 900 K in a 20% propane/He mixture. The spectrum for this sample after carburization loses its pre-edge feature, and the near-edge region appears in an energy range similar to that expected for Mo metal and Mo_2C (Figure 6), confirming that carbide species are formed. The spectrum, however, lacks the fine structure present in the spectrum of bulk Mo_2C , suggesting that the MoC_y species in the carburized Mo/H-ZSM5 sample do not have the long-range order required for these multiple scattering features. The radial structure function derived from the EXAFS of the carburized Mo-2 sample resembles that of the Mo-4 sample [8], indicating the formation of similar carbide species. FEFF fit of the radial structure function of the carburized sample requires the retention of Mo-O coordination, confirming that the bond with the framework oxygen remains after carburization.

The products formed during CH_4 reaction at 950 K were monitored using mass spectrometry (Figure 7). H_2 , CO, CO_2 , and H_2O (not shown) are the predominant initial products, and the total amount of oxygen removed as these products corresponds to 2.5 ± 0.2 for Mo/Al ratios between 0.11 and 0.48. This corresponds to the removal of all the oxygen

atoms in $(\text{Mo}_2\text{O}_5)^{2+}$ dimers without removal of the anchoring framework oxygen atoms. This is consistent with the infrared evidence that OH groups do not reappear after CH_4 treatment at 948 K. The retention of framework oxygen and of a Mo-O coordination between MoC_y and a framework oxygen are also consistent with cluster simulations of the fine structure XAS spectra of carburized Mo/H-ZSM5 samples [8]. The formation of hydrocarbons (e.g., benzene, ethylene) requires the removal of oxygen from the MoO_x precursors (Figure 7) and benzene formation rates reach a maximum after removal of about 1.5 O atoms per Mo. As oxygen continues to be removed, simultaneous carbon deposition causes the ultimate decrease in hydrocarbon formation rates [10].

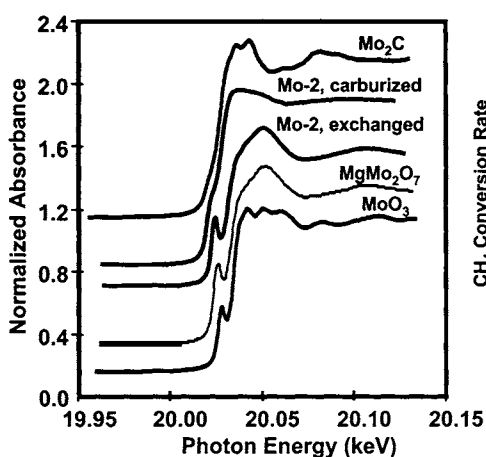


Figure 6. X-ray near edge spectra (XANES) of MoO_3 , MgMo_2O_7 , Mo_2C , and the Mo-2 sample ($\text{Mo}/\text{Al}_F = 0.26$) after solid-state exchange and after carburization.

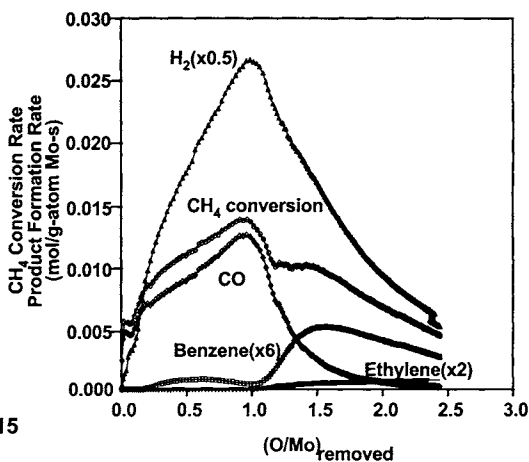


Figure 7. The CH_4 conversion rate and product formation rates during CH_4 reaction at 950 K, 100 ml/min 1:1 CH_4/Ar on the 2% wt. Mo/H-ZSM5 sample. The details of the procedure for data collection and analysis can be found in Ref. 10.

References

1. Solymosi, F., Cserenyi, J., Szoke, A., Bansagi, T., and Oszko, A., *J. Catal.* **165**, 150 (1997).
2. Borry, R.W., Lu, E.C., Kim, Y.H., and Iglesia, E., *Stud. Surf. Sci. Catal.* **119**, 403 (1998).
3. Weckhuysen, B.M., Wang, D., Rosynek, M.P., and Lunsford, J.H., *J. Catal.* **175**, 338 (1998).
4. Liu, S.T., Wang, L., Ohnishi, R., and Ichikawa, M., *J. Catal.* **181** (2), 175 (1999).
5. Liu, W. and Xu, Y., *J. Catal.* **185**, 386 (1999).
6. Wang, D., Lunsford, J.H., and Rosynek, M.P., *J. Catal.* **169**, 347 (1997).
7. Borry, R.W., Kim, Y.H., Huffsmith, A., Reimer, J.A., and Iglesia, E., *J. Phys. Chem.* **103**, 5787 (1999).
8. Li, W., Meitzner, G.D., Borry, R.W., and Iglesia, E., *J. Catal.*, submitted for publication (1999).
9. Zhang, J.Z., Long, M.A., and Howe, R.F., *Catal. Today* **44** (1-4), 293 (1998).
10. Kim, Y.H., Borry, R.W., and Iglesia, E., *Microporous Mater.*, in press (1999).
11. Ressler, T., *WinXAS 97*, version 1.2, 1998.
12. Zabinsky, S.I., Rehr, J.J., Ankudinov, A., Albers, R.C., and Eller, M.J., *Phys. Rev. B* **52**, 2995 (1995).
13. Pu, S.B. and Inui, T., *Zeolites* **19**, 452 (1997).
14. Campbell, S.M., Bibby, D.M., Coddington, J.M., Howe, R.F., and Meinhold, R.H., *J. Catal.* **161**, 338 (1996).
15. Weber, R.S., *J. Catal.* **151**, 470 (1995).
16. Verbruggen, N.F., Mestl, G., von Hippel, M.J., Lengeler, B., and Knozinger, H., *Langmuir* **10**, 3063 (1994).